

Nonsinglet parton distribution functions from the precise next-to-next-to-next-to leading order QCD fit

Ali N. Khorramian,^{1,2,*} H. Khanpour,^{1,†} and S. Atashbar Tehrani^{2,‡}

¹*Physics Department, Semnan University, P.O. Box 35195-363, Semnan, Iran*

²*School of Particles and Accelerators, Institute for Research in Fundamental Sciences (IPM)[§], P.O. Box 19395-5531, Tehran, Iran*

(Received 16 September 2009; published 14 January 2010)

We present the results of our QCD analysis for nonsinglet unpolarized quark distributions and structure function $F_2(x, Q^2)$ up to next-to-next-to-next-to leading order (N³LO). In this regards 4-loop anomalous dimension can be obtained from the Padé approximations. The analysis is based on the Jacobi polynomials expansion of the structure function. New parameterizations are derived for the nonsinglet quark distributions for the kinematic wide range of x and Q^2 . Our calculations for nonsinglet unpolarized quark distribution functions up to N³LO are in good agreement with available theoretical models. The higher twist contributions of $F_2^{p,d}(x, Q^2)$ are extracted in the large x region in N³LO analysis. The values of Λ_{QCD} and $\alpha_s(M_Z^2)$ are determined.

DOI: 10.1103/PhysRevD.81.014013

PACS numbers: 13.60.Hb, 12.39.-x, 14.65.Bt

I. INTRODUCTION

Structure functions in deep-inelastic scattering (DIS) and their scale evolution are closely related to the origins of quantum chromodynamics (QCD). DIS processes have played and still play a very important role for our understanding of QCD and nucleon structure [1]. In fact, DIS structure functions have been the subject of detailed theoretical and experimental investigations. Today, with high-precision data from the electron proton collider, HERA, and in view of the outstanding importance of hard scattering processes at proton-(anti)proton colliders like the TEVATRON and the forthcoming Large Hadron Collider (LHC) at CERN, a quantitative understanding of deep-inelastic processes is indispensable.

To predict the rates of the various processes, a set of universal parton distribution functions (PDFs) is required. On the other hand, all calculations of high energy processes with initial hadrons, whether within the standard model or exploring new physics, require PDFs as an essential input. The reliability of these calculations, which underpins both future theoretical and experimental progress, depends on understanding the uncertainties of the PDFs. These distribution functions can be determined by QCD global fits to all the available DIS and related hard-scattering data. The QCD fits can be performed at leading order (LO), next-to-leading order (NLO), next-to-next-to-leading order (N²LO) in the strong coupling α_s .

The assessment of PDFs, their uncertainties and extrapolation to the kinematics relevant for future colliders such as the LHC have been an important challenge to high energy physics in recent years. Over the last couple of years there

has been a considerable improvement in the precision and in the kinematic range of the experimental measurements for many of these processes, as well as new types of data becoming available. In addition, there have been valuable theoretical developments, which increase the reliability of the global analysis. It is therefore timely, particularly in view of the forthcoming experiments at the LHC at CERN, to perform new global analysis which incorporate all of these improvements. A lot of efforts and challenges have been done to obtain PDFs for the LHC [2] which take into account the higher order corrections [3–5].

For quantitatively reliable predictions of DIS and hard hadronic scattering processes, perturbative QCD corrections at the N²LO and the next-to-next-to-next-to-leading order (N³LO) need to be taken into account. Based on our experience obtained in a series of LO, NLO, and N²LO analysis [6] of the nonsinglet parton distribution functions, here we extend our work to N³LO accuracy in perturbative QCD.

In this work this important problem is studied with the help of the method of the structure function reconstruction over their Mellin moments, which is based on the expansion of the structure function in terms of Jacobi polynomials. This method was developed and applied for different QCD analyses [7–24]. The same method has also been applied in the polarized case in Refs. [25–30].

In the present paper we perform a QCD analysis of the flavor nonsinglet unpolarized deep-inelastic charged $e(\mu)p$ and $e(\mu)d$ world data [31–35] at N³LO and derived parameterizations of valence quark distributions $xu_v(x, Q^2)$ and $xd_v(x, Q^2)$ at a starting scale Q_0^2 together with the QCD scale Λ_{QCD} by using the Jacobi polynomial expansions. We have therefore used the 3-loop splitting functions and Padé approximations [36–40] for the evolution of nonsinglet quark distributions of hadrons.

Previous 3-loop QCD analysis were mainly performed as combined singlet and nonsinglet analysis [41,42], partly

*khorramiana@theory.ipm.ac.ir

†hamzeh_khanpour@nit.ac.ir

‡Atashbar@ipm.ir

§http://particles.ipm.ir/

based on preliminary, approximative expression of the 3-loop splitting functions. Other analyses were carried out for fixed moments only in the singlet and nonsinglet case analyzing neutrino data [43–45]. First results of the non-singlet analysis were published in [46]. Very recently a 3-loop nonsinglet analysis was also carried out in Refs. [6,47,48]. The results of 4-loop QCD analysis are also reported in [48,49]. The results of the present work are based on the Jacobi polynomials expansion of the non-singlet structure function.

The plan of the paper is to recall the theoretical formalism of the QCD analysis for calculating nonsinglet sector of proton structure function F_2 in Mellin- N space in Sec. II. Section III explains the Padé approximations and 4-loop anomalous dimensions. A description of the Jacobi polynomials and procedure of the QCD fit of F_2 data are illustrated in Sec. IV. The numerical results are illustrated in Sec. V before we summarize our findings in Sec. VI.

II. THEORETICAL FORMALISM OF THE QCD ANALYSIS

In the common $\overline{\text{MS}}$ factorization scheme the relevant F_2 structure function as extracted from the DIS ep process can be written as [50–53]

$$\begin{aligned} x^{-1}F_2(x, Q^2) &= x^{-1}(F_{2,\text{NS}}(x, Q^2) + F_{2,S}(x, Q^2) \\ &\quad + F_{2,g}(x, Q^2)) \\ &= C_{2,\text{NS}}(x, Q^2) \otimes q_{\text{NS}}(x, Q^2) \\ &\quad + \langle e^2 \rangle C_{2,S}(x, Q^2) \otimes q_S(x, Q^2) \\ &\quad + \langle e^2 \rangle C_{2,g}(x, Q^2) \otimes g(x, Q^2); \end{aligned} \quad (1)$$

here, q_i and g represent the quarks and gluons distributions, respectively. q_{NS} stands for the usual flavor nonsinglet combination and q_S stand for the flavor-singlet quark distribution, $q_S = \sum_{i=1}^{n_f} (q_i + \bar{q}_i)$. Also, n_f denotes the number of effectively massless flavors. $\langle e^2 \rangle$ represents the average squared charge, and \otimes denotes the Mellin convolution which turns into a simple multiplication in N space.

The perturbative expansion of the coefficient functions can be written as

$$C_{2,i}(x, \alpha_s(Q^2)) = \sum_{n=0} \left(\frac{\alpha_s(Q^2)}{4\pi} \right)^n C_{2,i}^{(n)}(x). \quad (2)$$

In LO, $C_{2,\text{NS}}^{(0)}(x) = \delta(x)$, $C_{2,\text{PS}}^{(0)}(x) = C_{2,g}^{(0)}(x) = C_{2,\text{PS}}^{(1)}(x) = 0$, and the singlet-quark coefficient function is decomposed into the nonsinglet and pure singlet contribution, $C_{2,q}^{(n)} \equiv C_{2,S}^{(n)} = C_{2,\text{NS}}^{(n)} + C_{2,\text{PS}}^{(n)}$. The coefficient functions $C_{2,i}^{(n)}$ up to $N^3\text{LO}$ have been given in [54].

The nonsinglet structure function $F_{2,\text{NS}}(x, Q^2)$ up to $N^3\text{LO}$ and for three active (light) flavors has the representation

$$\begin{aligned} x^{-1}F_{2,\text{NS}}(x, Q^2) &= [C_{2,q}^{(0)} + a_s C_{2,\text{NS}}^{(1)} + a_s^2 C_{2,\text{NS}}^{(2)+} + a_s^3 C_{2,\text{NS}}^{(3)+}] \\ &\quad \otimes \left[\frac{1}{18} q_8^+ + \frac{1}{6} q_3^+ \right](x, Q^2). \end{aligned} \quad (3)$$

The flavor-singlet and gluon contributions in Eq. (1) read

$$\begin{aligned} x^{-1}F_{2,S}(x, Q^2) &= \frac{2}{9} [C_{2,q}^{(0)} + a_s C_{2,q}^{(1)} + a_s^2 C_{2,q}^{(2)} + a_s^3 C_{2,q}^{(3)}] \\ &\quad \otimes \Sigma(x, Q^2); \end{aligned} \quad (4)$$

$$\begin{aligned} x^{-1}F_{2,g}(x, Q^2) &= \frac{2}{9} [a_s C_{2,g}^{(1)} + a_s^2 C_{2,g}^{(2)} + a_s^3 C_{2,g}^{(3)}] \\ &\quad \otimes g(x, Q^2). \end{aligned} \quad (5)$$

The symbol \otimes denotes the Mellin convolution

$$[A \otimes B](x) = \int_0^1 dx_1 \int_0^1 dx_2 \delta(x - x_1 x_2) A(x_1) B(x_2). \quad (6)$$

In Eq. (3) $q_3^+ = u + \bar{u} - (d + \bar{d}) = u_v - d_v$ and $q_8^+ = u + \bar{u} + d + \bar{d} - 2(s + \bar{s}) = u_v + d_v + 2\bar{u} + 2\bar{d} - 4\bar{s}$, where $s = \bar{s}$. Also in Eq. (4), $\Sigma(x, Q^2) \equiv \sum_{q=u,d,s} (q + \bar{q}) = u_v + d_v + 2\bar{u} + 2\bar{d} + 2\bar{s}$. Notice that in the above equations $a_s = a_s(Q^2) \equiv \alpha_s(Q^2)/4\pi$ denotes the strong coupling constant and $C_{i,j}$ are the Wilson coefficients [54].

The combination of parton densities in the nonsinglet regime and the valence region $x \geq 0.3$ for F_2^p in LO is

$$\frac{1}{x} F_2^p(x, Q^2) = \left[\frac{1}{18} q_{\text{NS},8}^+ + \frac{1}{6} q_{\text{NS},3}^+ \right](x, Q^2) + \frac{2}{9} \Sigma(x, Q^2), \quad (7)$$

where $q_{\text{NS},3}^+ = u_v - d_v$, $q_{\text{NS},8}^+ = u_v + d_v$, and $\Sigma = u_v + d_v$, since sea quarks can be neglected in the region $x \geq 0.3$. So in the x space we have

$$\begin{aligned} F_2^p(x, Q^2) &= \left(\frac{5}{18} x q_{\text{NS},8}^+ + \frac{1}{6} x q_{\text{NS},3}^+ \right)(x, Q^2) \\ &= \frac{4}{9} x u_v(x, Q^2) + \frac{1}{9} x d_v(x, Q^2). \end{aligned} \quad (8)$$

In the above region the combinations of parton densities for F_2^d are also given by

$$F_2^d(x, Q^2) = \left(\frac{5}{18} x q_{\text{NS},8}^+ \right)(x, Q^2) = \frac{5}{18} x (u_v + d_v)(x, Q^2), \quad (9)$$

where $q_{\text{NS},3}^+ = u_v - d_v$ and $F_2^d = (F_2^p + F_2^n)/2$ if we ignore the nuclear effects here. It is important to stress that the shadowing effect as a nuclear effect may affect our analysis. The shadowing effect [55,56] arising from the gluon recombination and in the small- x region, the competitive mechanism of nuclear shadowing takes place. It also depends on the size of the nucleons. According to this effect we have $F_2^d = (F_2^p + F_2^n)/2 + \delta F_2^d$. To obtain the δF_2^d we need to know the generalized vector meson dominance (VMD) and parton mechanism at low and large

values of Q^2 , respectively. We found that the value of δF_2^d is important but in low values of x . For example, this correction value at $Q^2 = 10 \text{ GeV}^2$ and for $x > 0.1$ is too small ($\sim 10^{-4}$). So in the valence region of this analysis, this effect is negligible in large x and we can use the $F_2^d = (F_2^p + F_2^n)/2$ approximately.

In the region $x \leq 0.3$ for the difference of the proton and deuteron data we use

$$\begin{aligned} F_2^{\text{NS}}(x, Q^2) &\equiv 2(F_2^p - F_2^d)(x, Q^2) = \frac{1}{3}xq_{\text{NS},3}^+(x, Q^2) \\ &= \frac{1}{3}x(u_v - d_v)(x, Q^2) + \frac{2}{3}x(\bar{u} - \bar{d})(x, Q^2), \end{aligned} \quad (10)$$

where now $q_{\text{NS},3}^+ = u_v - d_v + 2(\bar{u} - \bar{d})$ since sea quarks cannot be neglected for x smaller than about 0.3.

The first clear evidence for the flavor asymmetry combination of light parton distributions $x(\bar{d} - \bar{u})$ in nature came from the analysis of NMC at CERN to study of the Gottfried sum rule [57]. In our calculation we supposed the $\bar{d} - \bar{u}$ distribution [47,48,58,59]

$$\begin{aligned} x(\bar{d} - \bar{u})(x, Q_0^2) &= 1.195x^{1.24}(1-x)^{9.10}(1+14.05x \\ &\quad - 45.52x^2), \end{aligned} \quad (11)$$

at $Q_0^2 = 4 \text{ GeV}^2$ which gives a good description of the

Drell-Yan dimuon production data [60]. In this analysis, like other analyses [6,17,47,48,58,59], we used the above distribution for considering the symmetry breaking of sea quarks. Although, in fact, this parametrization plays a marginal role in our analysis, in order to find the impact effect of this distribution, which is essentially used in the paper, it is desirable to study the QCD fits by varying this distribution with another asymmetry sea quark distribution which is derived in other analyses. In Sec. VI we will discuss our outputs when we change the above sea distribution.

Now these results in the physical region $0 < x \leq 1$ can transform to Mellin- N space by using the Mellin transform to obtain the moments of the structure function as $\frac{1}{x}F_2^k$,

$$F_2^k(N, Q^2) \equiv \mathbf{M}[F_2^k, N] = \int_0^1 dx x^{N-1} \frac{1}{x} F_2^k(x, Q^2); \quad (12)$$

here k denotes the three above cases, i.e. $k = p, d, \text{NS}$. One of the advantages of Mellin-space calculations is the fact that the Mellin transform of a convolution of functions in Eqs. (3)–(5) reduces to a simple product

$$\mathbf{M}[A \otimes B, N] = \mathbf{M}[A, N]\mathbf{M}[B, N] = A(N)B(N). \quad (13)$$

By using the solution of the nonsinglet evolution equation for the parton densities to 4-loop order, the nonsinglet structure functions are given by [48]

$$\begin{aligned} F_2^k(N, Q^2) &= (1 + a_s C_{2,\text{NS}}^{(1)}(N) + a_s^2 C_{2,\text{NS}}^{(2)}(N) + a_s^3 C_{2,\text{NS}}^{(3)}(N)) F_2^k(N, Q_0^2) \left(\frac{a_s}{a_0}\right)^{-\hat{P}_0(N)/\beta_0} \left\{ 1 - \frac{1}{\beta_0}(a_s - a_0) \left[\hat{P}_1^+(N) - \frac{\beta_1}{\beta_0} \hat{P}_0(N) \right] \right. \\ &\quad - \frac{1}{2\beta_0}(a_s^2 - a_0^2) \left[\hat{P}_2^+(N) - \frac{\beta_1}{\beta_0} \hat{P}_1^+(N) + \left(\frac{\beta_1^2}{\beta_0^2} - \frac{\beta_2}{\beta_0}\right) \hat{P}_0(N) \right] + \frac{1}{2\beta_0^2}(a_s - a_0)^2 \left(\hat{P}_1^+(N) - \frac{\beta_1}{\beta_0} \hat{P}_0(N) \right)^2 \\ &\quad - \frac{1}{3\beta_0}(a_s^3 - a_0^3) \left[\hat{P}_3^+(N) - \frac{\beta_1}{\beta_0} \hat{P}_2^+(N) + \left(\frac{\beta_1^2}{\beta_0^2} - \frac{\beta_2}{\beta_0}\right) \hat{P}_1^+(N) + \left(\frac{\beta_1^3}{\beta_0^3} - 2\frac{\beta_1\beta_2}{\beta_0^2} + \frac{\beta_3}{\beta_0}\right) \hat{P}_0(N) \right] \\ &\quad + \frac{1}{2\beta_0^2}(a_s - a_0)(a_0^2 - a_s^2) \left(\hat{P}_1^+(N) - \frac{\beta_1}{\beta_0} \hat{P}_0(N) \right) \left[\hat{P}_2(N) - \frac{\beta_1}{\beta_0} \hat{P}_1(N) - \left(\frac{\beta_1^2}{\beta_0^2} - \frac{\beta_2}{\beta_0}\right) \hat{P}_0(N) \right] \\ &\quad \left. - \frac{1}{6\beta_0^3}(a_s - a_0)^3 \left(\hat{P}_1^+(N) - \frac{\beta_1}{\beta_0} \hat{P}_0(N) \right)^3 \right\}. \end{aligned} \quad (14)$$

Here $a_s (= \alpha_s/4\pi)$ and a_0 denotes the strong coupling constant in the scale of Q^2 and Q_0^2 , respectively. $k = p, d$ and NS also denotes the three above cases, i.e. proton, deuteron, and nonsinglet structure function. $C_{2,\text{NS}}^{(m)}(N)$ are the nonsinglet Wilson coefficients in $O(a_s^m)$ which can be found in [54,61,62] and \hat{P}_m denote also the Mellin transforms of the $(m+1)$ -loop splitting functions.

III. PADÉ APPROXIMATIONS AND 4-LOOP ANOMALOUS DIMENSIONS

In spite of the unknown 4-loop anomalous dimensions, one can obtain the nonsinglet parton distributions and Λ_{QCD} by estimating uncalculated fourth-order corrections

to the nonsinglet anomalous dimension. On the other hand, the 3-loop Wilson coefficients are known [54] and now it is possible to know which effect has the 4-loop anomalous dimension if compared to the Wilson coefficient. In this case the 4-loop anomalous dimension may be obtained from Padé approximations.

Padé approximations have proved to be useful in many physical applications. Padé approximations may be used either to predict the next term in some perturbative series, called a Padé approximation prediction, or to estimate the sum of the entire series, called Padé summation.

For this purpose we use the Padé approximations of the perturbative series, discussed in detail for QCD, e.g., in Refs. [36–38]. Padé approximations [39,40] are rational

functions chosen to equal the perturbative series to the order calculated:

$$[\mathcal{N}/\mathcal{M}] = \frac{a_0 + a_1x + \dots + a_{\mathcal{N}}x^{\mathcal{N}}}{1 + b_1x + \dots + b_{\mathcal{M}}x^{\mathcal{M}}}, \quad (15)$$

to the series

$$S = S_0 + S_1x + \dots + S_{\mathcal{N}+\mathcal{M}}x^{\mathcal{N}+\mathcal{M}}, \quad (16)$$

where we set

$$[\mathcal{N}/\mathcal{M}] = S + \mathcal{O}(x^{\mathcal{N}+\mathcal{M}+1}),$$

and write an equation for the coefficients of each power of x . To continue, let's go to Mellin- N space.

A generic QCD anomalous dimension expansion in term of a_s then may be written in the form

$$\gamma(N) = \sum_{l=0}^{\infty} a_s^{l+1} \gamma^{(l)}(N). \quad (17)$$

In Mellin- N space and by using this approach we can replace $\gamma(N)$ by a rational function in a_s [54],

$$\begin{aligned} \tilde{\gamma}^{[\mathcal{N}/\mathcal{M}]}(N) &\equiv [\mathcal{N}/\mathcal{M}](N) \\ &= \frac{p_0 + a_s p_1(N) + \dots + a_s^{\mathcal{N}} p_{\mathcal{N}}(N)}{1 + a_s q_1(N) + \dots + a_s^{\mathcal{M}} q_{\mathcal{M}}(N)}. \end{aligned} \quad (18)$$

Here $\mathcal{M} \geq 1$ and $\mathcal{N} + \mathcal{M} = n$, where n stands for the maximal order in a_s at which the expansion coefficients $\gamma^{(n)}(N)$ have been determined from an exact calculation. The functions $p_i(N)$ and $q_j(N)$ are determined from these known coefficients by expanding Eq. (18) in powers of a_s . This expansion then also provides the $[\mathcal{N}/\mathcal{M}]$ Padé approximate for the $(n+1)$ -th order quantities $\gamma^{(n+1)}$.

In this way it is easy to obtain the following results for $\mathcal{M} = \mathcal{N} = 1$ and for $\mathcal{M} = 0, \mathcal{N} = 2$

$$\begin{aligned} \tilde{\gamma}^{[1/1]}(N) &\equiv [1/1](N) = \frac{\gamma^{(2)}(N)}{\gamma^{(1)}(N)}, \\ \tilde{\gamma}^{[0/2]}(N) &\equiv [0/2](N) = \frac{2\gamma^{(1)}(N)\gamma^{(2)}(N)}{\gamma^{(0)}(N)} - \frac{\gamma^{(1)^3}(N)}{\gamma^{(0)^2}(N)}. \end{aligned} \quad (19)$$

The strong coupling constant a_s plays a more central role in the present paper to the evolution of parton densities. At N^m LO the scale dependence of a_s is given by

$$\frac{da_s}{d \ln Q^2} = \beta_{N^m \text{LO}}(a_s) = - \sum_{k=0}^m a_s^{k+2} \beta_k. \quad (20)$$

The expansion coefficients β_k of the β function of QCD are known up to $k = 3$, i.e., N^3 LO [63,64]

$$\begin{aligned} \beta_0 &= 11 - 2/3n_f, & \beta_1 &= 102 - 38/3n_f, \\ \beta_2 &= 2857/2 - 5033/18n_f + 325/54n_f^2, \\ \beta_3 &= 29243.0 - 6946.30n_f + 405.089n_f^2 + 1093/729n_f^3, \end{aligned} \quad (21)$$

here n_f stands for the number of effectively massless quark flavors and β_k denote the coefficients of the usual four-dimensional $\overline{\text{MS}}$ beta function of QCD. In complete 4-loop approximation and using the Λ -parametrization, the running coupling is given by [65,66]

$$\begin{aligned} a_s(Q^2) &= \frac{1}{\beta_0 L_\Lambda} - \frac{1}{(\beta_0 L_\Lambda)^2} b_1 \ln L_\Lambda + \frac{1}{(\beta_0 L_\Lambda)^3} [b_1^2 (\ln^2 L_\Lambda \\ &\quad - \ln L_\Lambda - 1) + b_2] + \frac{1}{(\beta_0 L_\Lambda)^4} \left[b_1^3 \left(-\ln^3 L_\Lambda \right. \right. \\ &\quad \left. \left. + \frac{5}{2} \ln^2 L_\Lambda + 2 \ln L_\Lambda - \frac{1}{2} \right) - 3b_1 b_2 \ln L_\Lambda + \frac{b_3}{2} \right], \end{aligned} \quad (22)$$

where $L_\Lambda \equiv \ln(Q^2/\Lambda^2)$, $b_k \equiv \beta_k/\beta_0$, and Λ is the QCD scale parameter. The first line of Eq. (22) includes the 1- and the 2-loop coefficients, the second line is the 3-loop, and the third line denotes the 4-loop correction. Equation (22) solves the evolution equation (20) only up to higher orders in $1/L_\Lambda$. The functional form of $\alpha_s(Q^2)$, in 4-loop approximation and for 6 different values of Λ , is

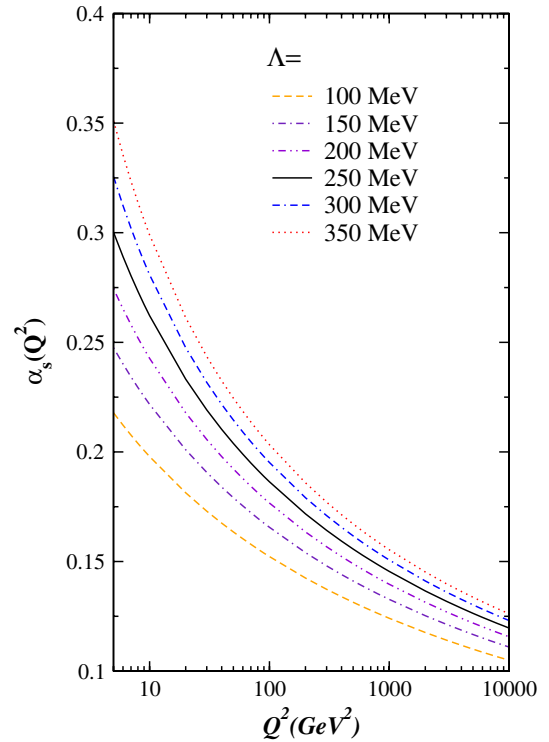


FIG. 1 (color online). The strong running of $\alpha_s(Q^2)$, according to Eq. (22), in 4-loop approximation and for different values of Λ .

displayed in Fig. 1. The slope and dependence on the actual value of Λ is especially pronounced at small Q^2 , while at large Q^2 both the energy dependence and the dependence on Λ becomes increasingly feeble. To be able to compare with other measurements of Λ we adopt the matching of flavor thresholds at $Q^2 = m_c^2$ and $Q^2 = m_b^2$ with $m_c = 1.5$ GeV and $m_b = 4.5$ GeV as described in [67,68].

IV. JACOBI POLYNOMIALS AND THE PROCEDURE OF QCD FITS

One of the simplest and fastest possibilities in the structure function reconstruction from the QCD predictions for its Mellin moments is Jacobi polynomials expansion. The Jacobi polynomials are especially suitable for this purpose since they allow one to factor out an essential part of the x dependence of structure function into the weight function [8].

According to this method, one can relate the F_2 structure function with its Mellin moments

$$F_2^{k,N_{\max}}(x, Q^2) = x^\beta(1-x)^\alpha \sum_{n=0}^{N_{\max}} \Theta_n^{\alpha,\beta}(x) \times \sum_{j=0}^n c_j^{(n)}(\alpha, \beta) F_2^k(j+2, Q^2), \quad (23)$$

where N_{\max} is the number of polynomials, k denotes the three cases, i.e. $k = p, d, \text{NS}$. Jacobi polynomials of order n [69], $\Theta_n^{\alpha,\beta}(x)$, satisfy the orthogonality condition with the weight function $w^{\alpha\beta} = x^\beta(1-x)^\alpha$

$$\int_0^1 dx w^{\alpha\beta} \Theta_k^{\alpha,\beta}(x) \Theta_l^{\alpha,\beta}(x) = \delta_{k,l}. \quad (24)$$

In the above, $c_j^{(n)}(\alpha, \beta)$ are the coefficients expressed through Γ functions and satisfying the orthogonality relation in Eq. (24), and $F_2(j+2, Q^2)$ are the moments determined in the previous section. N_{\max} , α and β have to be chosen so as to achieve the fastest convergence of the series on the right-hand side of Eq. (23) and to reconstruct F_2 with the required accuracy. In our analysis we use $N_{\max} = 9$, $\alpha = 3.0$, and $\beta = 0.5$. The same method has been applied to calculate the nonsinglet structure function $x F_3$ from their moments [13–16] and for polarized structure function $x g_1$ [25–27]. Obviously the Q^2 dependence of the polarized structure function is defined by the Q^2 dependence of the moments.

The evolution equations allow one to calculate the Q^2 dependence of the parton distributions provided at a certain reference point Q_0^2 . These distributions are usually parameterized on the basis of plausible theoretical assumptions concerning their behavior near the end points $x = 0, 1$.

In the present analysis we choose the following parametrization for the valence quark densities in the input scale of $Q_0^2 = 4$ GeV²:

$$xq_v(x, Q_0^2) = \mathcal{N}_q x^{a_q} (1-x)^{b_q} (1 + c_q \sqrt{x} + d_q x), \quad (25)$$

where $q = u, d$ and the normalization factors \mathcal{N}_u and \mathcal{N}_d are fixed by $\int_0^1 u_v dx = 2$ and $\int_0^1 d_v dx = 1$, respectively. By QCD fits of the world data for $F_2^{p,d}$, we can extract valence quark densities using the Jacobi polynomials method. For the nonsinglet QCD analysis presented in this paper we use the structure function data measured in charged lepton-proton and deuteron deep-inelastic scattering. The experiments contributing to the statistics are BCDMS [31], SLAC [32], NMC [33], H1 [34], and ZEUS [35]. In our QCD analysis we use three data samples: $F_2^p(x, Q^2)$, $F_2^d(x, Q^2)$ in the nonsinglet regime and the valence quark region $x \geq 0.3$, and $F_2^{\text{NS}} = 2(F_2^p - F_2^d)$ in the region $x < 0.3$.

The valence quark region may be parameterized by the nonsinglet combinations of parton distributions, which are expressed through the parton distributions of valence quarks. Only data with $Q^2 > 4$ GeV² were included in the analysis and a cut in the hadronic mass of $W^2 \equiv (\frac{1}{x} - 1)Q^2 + m_N^2 > 12.5$ GeV² was applied in order to widely eliminate higher twist (HT) effects from the data samples. After these cuts we are left with 762 data points, 322 for F_2^p , 232 for F_2^d , and 208 for F_2^{NS} . By considering the additional cuts on the BCDMS ($y > 0.35$) and on the NMC data ($Q^2 > 8$ GeV²) the total number of data points available for the analysis reduce from 762 to 551, because we have 227 data points for F_2^p , 159 for F_2^d , and 165 for F_2^{NS} .

For data used in the global analysis, most experiments combine various systematic errors into one effective error for each data point, along with the statistical error. In addition, the fully correlated normalization error of the experiment is usually specified separately. For this reason, it is natural to adopt the following definition for the effective χ^2 [6,70]

$$\chi_{\text{global}}^2 = \sum_n w_n \chi_n^2 \quad (n \text{ labels the different experiments})$$

$$\chi_n^2 = \left(\frac{1 - \mathcal{N}_n}{\Delta \mathcal{N}_n} \right)^2 + \sum_i \left(\frac{\mathcal{N}_n F_{2,i}^{\text{data}} - F_{2,i}^{\text{theor}}}{\mathcal{N}_n \Delta F_{2,i}^{\text{data}}} \right)^2. \quad (26)$$

For the n th experiment, $F_{2,i}^{\text{data}}$, $\Delta F_{2,i}^{\text{data}}$, and $F_{2,i}^{\text{theor}}$ denote the data value, measurement uncertainty (statistical and systematic combined), and theoretical value for the i th data point. $\Delta \mathcal{N}_n$ is the experimental normalization uncertainty and \mathcal{N}_n is an overall normalization factor for the data of experiment n . The factor w_n is a possible weighting factor (with default value 1). However, we allowed for a relative normalization shift \mathcal{N}_n between the different data sets within the normalization uncertainties $\Delta \mathcal{N}_n$ quoted by the experiments. For example the normalization uncertainty of the NMC (combined) data is estimated to be 2.5%. The normalization shifts \mathcal{N}_n were fitted once and then kept fixed.

Now the sums in χ_{global}^2 run over all data sets and in each data set over all data points. The minimization of the above χ^2 value to determine the best parametrization of the unpolarized parton distributions is done using the program MINUIT [71].

The one σ error for the parton density xq_v as given by Gaussian error propagation is [48]

$$\sigma(xq_v(x))^2 = \sum_{i=1}^{n_p} \sum_{j=1}^{n_p} \left(\frac{\partial xq_v}{\partial p_i} \right) \left(\frac{\partial xq_v}{\partial p_j} \right) \text{cov}(p_i, p_j), \quad (27)$$

where the sum runs over all fitted parameters. The functions $\partial xq_v/\partial p_i$ are the derivatives of xq_v with respect to the fit parameter p_i , and $\text{cov}(p_i, p_j)$ are the elements of the covariance matrix. The derivatives $\partial xq_v/\partial p_i$ can be calculated analytically at the input scale Q_0^2 . Their values at Q^2 are given by evolution which is performed in Mellin- N space.

Now we need to discuss the derivatives in Mellin- N space a bit further. The Mellin- N moment for complex values of N calculated at the input scale Q_0^2 for the parton density parameterized as in Eq. (25) is given by

$$q_v(N, a_q, b_q, c_q, d_q) = \mathcal{N}_q \mathbf{M}(n, a_q, b_q, c_q, d_q), \quad (28)$$

with the normalization constant

$$\mathcal{N}_q = \frac{C_{q_v}}{\mathbf{M}(1, a_q, b_q, c_q, d_q)}. \quad (29)$$

Here C_{q_v} is the respective number of valence quarks, i.e. $C_{u_v} = 2$ and $C_{d_v} = 1$. In the above $\mathbf{M}(n, a_q, b_q, c_q, d_q)$ is given by

$$\begin{aligned} \mathbf{M}(n, a_q, b_q, c_q, d_q) &= B[a_q + n - 1, b_q + 1] \\ &+ c_q B[a + n + 1/2, b + 1] \\ &+ d_u B[a_q + n, b_q + 1], \end{aligned} \quad (30)$$

where $B[a, b]$ denotes the Euler beta function for complex arguments. The general form of the derivative of the Mellin moment q_v with respect to the parameter p is given by

$$\frac{\partial q_v(N, p)}{\partial p} = \mathbf{M}(n, p) \frac{\partial \mathcal{N}_q}{\partial p} + \mathcal{N}_q \frac{\partial \mathbf{M}(n, p)}{\partial p}. \quad (31)$$

In this analysis only the parameters a_q and b_q have been fitted for both the xu_v and xd_v parametrization while the other parameters involved are kept fixed after a first minimization in the MINUIT program, since their errors turned out to be rather large compared to the central values. Here we want to show the derivatives u_v and d_v parton densities with respect to parameter a_q and b_q . For example,

$$\begin{aligned} f(n, a_q) &\equiv \frac{\partial \mathbf{M}(n, a_q)}{\partial a_q} \\ &= B[a_q + n - 1, b_q + 1] (\psi[a_q + n - 1] \\ &\quad - \psi[a_q + b_q + n]) + c_q B[a_q + n - 1/2, b_q + 1] \\ &\quad \times (\psi[a_q + n - 1/2] - \psi[a + b + n + 1/2]) \\ &\quad + d_q B[a_q + n, b_q + 1] (\psi[a_q + n] \\ &\quad - \psi[a_q + b_q + n + 1]), \end{aligned} \quad (32)$$

$$\begin{aligned} f(n, b_q) &\equiv \frac{\partial \mathbf{M}(n, b_q)}{\partial b_q} \\ &= B[a_q + n - 1, b_q + 1] (\psi[b_q + 1] \\ &\quad - \psi[a_q + b_q + n]) + c_q B[a_q + n - 1/2, b_q + 1] \\ &\quad \times (\psi[1 + b_q] - \psi[a_q + b_q + n + 1/2]) \\ &\quad + d_q B[a_q + n, b_q + 1] (\psi[b_q + 1] \\ &\quad - \psi[a_q + b_q + n + 1]), \end{aligned} \quad (33)$$

and now we can reach the below derivatives for $u_v(N)$ and $d_v(N)$ with respect to parameters a_q and b_q

$$\frac{\partial q_v(N, p)}{\partial p} = \mathcal{N}_q (f(n, p) - f(1, p) \mathbf{M}(n, p) / \mathbf{M}(1, p)), \quad (34)$$

also $\psi[n] = d \ln \Gamma(n) / dn$ is Euler's ψ function.

To obtain the error calculation of the structure functions F_2^p , F_2^d , and F_2^{NS} the relevant gradients of the PDFs in Mellin space have to be multiplied with the corresponding Wilson coefficients. This yields the errors as far as the QCD parameter Λ is fixed and regarded uncorrelated. The error calculation for a variable Λ is done numerically due to the nonlinear relation and required iterative treatment in the calculation of $\alpha_s(Q^2, \Lambda)$ [6,48].

V. RESULTS

In the QCD analysis of the present paper we used three data sets: the structure functions $F_2^p(x, Q^2)$ and $F_2^d(x, Q^2)$ in the region of $x \geq 0.3$, and the combination of these structure functions $F_2^{\text{NS}}(x, Q^2)$ in the region of $x < 0.3$. Notice that we take into account the cuts $Q^2 > 4 \text{ GeV}^2$, $W^2 > 12.5 \text{ GeV}^2$ for our QCD fits to determine some unknown parameters. In Fig. 2 the proton, deuteron, and nonsinglet data for $F_2^p(x, Q^2)$, $F_2^d(x, Q^2)$, and $F_2^{\text{NS}}(x, Q^2)$ are shown in the nonsinglet regime and the valence quark region $x \geq 0.3$ indicating the above cuts by a vertical dashed line. The solid lines correspond to the N³LO QCD fit. Now, it is possible to take into account the target

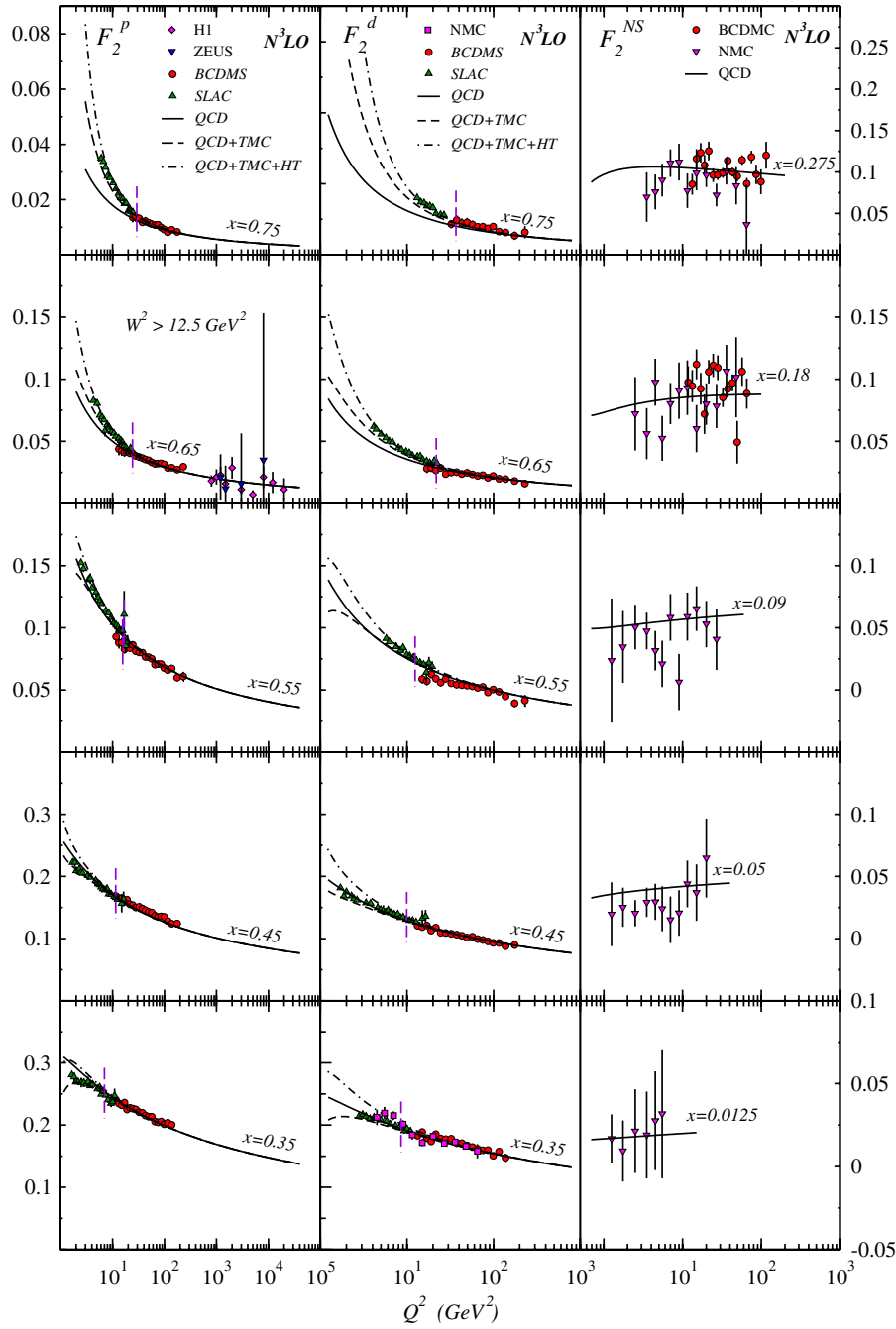


FIG. 2 (color online). The structure functions F_2^p , F_2^d , and F_2^{NS} as a function of Q^2 in intervals of x . Shown are the Padé [1/1] QCD fits in N^3LO (solid line) and the contributions from target mass corrections (dashed line) and higher twist (dash-dotted line). The vertical dashed line indicates the regions with $W^2 > 12.5 \text{ GeV}^2$.

mass effects in our calculations. The perturbative form of the moments is derived under the assumption that the mass of the target hadron is zero (in the limit $Q^2 \rightarrow \infty$). At intermediate and low Q^2 this assumption will begin to break down and the moments will be subject to potentially significant power corrections, of order $\mathcal{O}(m_N^2/Q^2)$, where m_N is the mass of the nucleon. These are known as target mass corrections (TMCs) and when included, the moments of flavor nonsinglet structure function have the form [47,72]

$$\begin{aligned}
 F_{2,\text{TMC}}^k(n, Q^2) &\equiv \int_0^1 x^{n-1} \frac{1}{x} F_{2,\text{TMC}}^k(x, Q^2) dx \\
 &= F_2^k(n, Q^2) + \frac{n(n-1)}{n+2} \left(\frac{m_N^2}{Q^2} \right) F_2^k(n+2, Q^2) \\
 &\quad + \frac{(n+2)(n+1)n(n-1)}{2(n+4)(n+3)} \left(\frac{m_N^2}{Q^2} \right)^2 \\
 &\quad \times F_2^k(n+4, Q^2) + \mathcal{O}\left(\frac{m_N^2}{Q^2}\right)^3, \quad (35)
 \end{aligned}$$

where higher powers than $(m_N^2/Q^2)^2$ are negligible for the relevant $x < 0.8$ region. By inserting Eq. (35) in Eq. (23) we have

$$F_2^{k,N_{\max}}(x, Q^2) = x^\beta(1-x)^\alpha \sum_{n=0}^{N_{\max}} \Theta_n^{\alpha,\beta}(x) \times \sum_{j=0}^n c_j^{(n)} \times (\alpha, \beta) F_{2,\text{TMC}}^k(j+2, Q^2), \quad (36)$$

where $F_{2,\text{TMC}}^k(j+2, Q^2)$ are the moments determined by Eq. (35). In Fig. 2 the dashed lines correspond to the N³LO QCD fit adding target mass corrections.

Despite the kinematic cuts ($Q^2 \geq 4 \text{ GeV}^2$, $W^2 \equiv (\frac{1}{x} - 1)Q^2 + m_N^2 \geq 12.5 \text{ GeV}^2$) used for our analysis, we also take into account higher twist corrections to $F_2^p(x, Q^2)$ and $F_2^d(x, Q^2)$ in the kinematic region $Q^2 \geq 4 \text{ GeV}^2$, $4 < W^2 < 12.5 \text{ GeV}^2$ in order to learn whether nonperturbative effects may still contaminate our perturbative analysis. For this purpose we extrapolate the QCD fit results obtained for $W^2 \geq 12.5 \text{ GeV}^2$ to the region $Q^2 \geq 4 \text{ GeV}^2$, $4 < W^2 < 12.5 \text{ GeV}^2$ and from the difference between data and theory, applying target mass corrections in addition. Now by considering higher twist correction

$$F_2^{\text{exp}}(x, Q^2) = O_{\text{TMC}}[F_2^{\text{HT}}(x, Q^2)] \cdot \left(1 + \frac{h(x, Q^2)}{Q^2 [\text{GeV}^2]}\right), \quad (37)$$

the higher twist coefficient can be extract. Here the operation $O_{\text{TMC}}[\dots]$ denotes taking the target mass corrections of the twist-2 contributions to the respective structure function. The coefficients $h(x, Q^2)$ are determined in bins of x and Q^2 and are then averaged over Q^2 . We extrapolate our QCD fits to the region $12.5 \text{ GeV}^2 \geq W^2 \geq 4 \text{ GeV}^2$ in Fig. 2. The dash-dotted lines in this figure correspond to the N³LO QCD fit adding target mass and higher twist corrections. There, at higher values of x a clear gap between the data and the QCD fit is seen.

In Table I we summarize the NLO, N²LO, and N³LO with using Padé [1/1] and [0/2] fit results for the parameters of the parton densities $xu_v(x, Q_0^2)$, $xd_v(x, Q_0^2)$, and $\Lambda_{\text{QCD}}^{N_f=4}$. The values without error have been fixed after a first minimization since the data do not constrain these parameters well enough. In this table we also compare the N³LO results with the NLO and N²LO results from Ref. [6]. The results show a good compatibility between Padé [1/1] and [0/2] approximations in 4-loop order. The resulted value of χ^2/ndf is 0.9578 at NLO, 0.9267 at N²LO, and 0.8994 and 0.8995 for Padé [1/1] and [0/2], respectively, at N³LO. Our results for the covariance matrix of the N³LO nonsinglet QCD fit for Padé [1/1] and [0/2] are presented in Table II.

TABLE I. Parameter values of the NLO, N²LO from Ref. [6] and N³LO nonsinglet QCD fit at $Q_0^2 = 4 \text{ GeV}^2$ for Padé [1/1] and Padé [0/2].

		NLO	N ² LO	N ³ LO Padé [1/1]	N ³ LO Padé [0/2]
u_v	a_u	0.7434 ± 0.009	0.7772 ± 0.009	0.79167 ± 0.0106	0.79176 ± 0.0099
	b_u	3.8907 ± 0.040	4.0034 ± 0.033	4.02637 ± 0.0402	4.02685 ± 0.0327
	c_u	0.1620	0.1000	0.0940	0.0940
	d_u	1.2100	1.1400	1.1100	1.1100
d_v	a_d	0.7369 ± 0.040	0.7858 ± 0.043	0.80927 ± 0.0621	0.80927 ± 0.0407
	b_d	3.5051 ± 0.225	3.6336 ± 0.244	3.76847 ± 0.3499	3.76858 ± 0.2278
	c_d	0.3899	0.1838	0.1399	0.1399
	d_d	-1.3700	-1.2152	-1.1200	-1.1200
$\Lambda_{\text{QCD}}^{N_f=4}, \text{ MeV}$		263.8 ± 30	239.9 ± 27	241.44 ± 29	241.45 ± 27
χ^2/ndf		$523/546 = 0.9578$	$506/546 = 0.9267$	$491.07/546 = 0.8994$	$491.12/546 = 0.8995$

TABLE II. Our results for the covariance matrix of the N³LO nonsinglet QCD fit for Padé [1/1] and [0/2] at $Q_0^2 = 4 \text{ GeV}^2$ by using MINUIT [71].

N ³ LO Padé [1/1]	a_u	b_u	a_d	b_d	$\Lambda_{\text{QCD}}^{N_f=4}$
a_u	1.13×10^{-4}				
b_u	2.35×10^{-4}	1.62×10^{-3}			
a_d	1.09×10^{-4}	-1.59×10^{-3}	3.86×10^{-3}		
b_d	1.67×10^{-4}	-8.84×10^{-3}	2.11×10^{-2}	1.23×10^{-1}	
$\Lambda_{\text{QCD}}^{(4)}$	1.71×10^{-4}	-3.49×10^{-4}	5.04×10^{-4}	2.61×10^{-3}	8.65×10^{-4}
N ³ LO Padé [0/2]	a_u	b_u	a_d	b_d	$\Lambda_{\text{QCD}}^{N_f=4}$
a_u	0.98×10^{-4}				
b_u	1.83×10^{-4}	1.07×10^{-3}			
a_d	-5.07×10^{-5}	-6.01×10^{-4}	1.66×10^{-3}		
b_d	-1.11×10^{-4}	-3.30×10^{-3}	8.58×10^{-3}	5.19×10^{-2}	
$\Lambda_{\text{QCD}}^{(4)}$	1.59×10^{-4}	-1.99×10^{-4}	1.94×10^{-4}	8.07×10^{-4}	7.53×10^{-4}

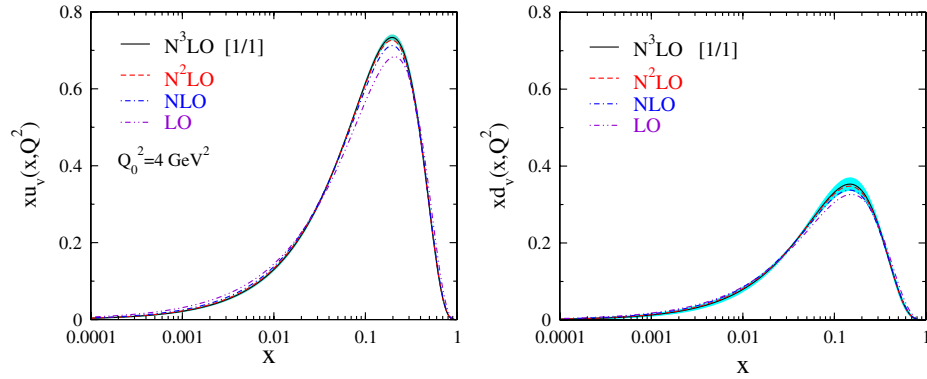


FIG. 3 (color online). The parton densities xu_v and xd_v up to 4-loop (Padé [1/1]) at the input scale $Q_0^2 = 4.0 \text{ GeV}^2$ (solid line) compared with results obtained from $N^2\text{LO}$ analysis (dashed-line), NLO analysis (dash-dotted line), and LO analysis (dash-dot-dotted line) [6]. The shaded areas represent the fully correlated one σ statistical error bands.

Figure 3 illustrates our fit results for $xu_v(x, Q_0^2)$, $xd_v(x, Q_0^2)$ at $Q_0^2 = 4 \text{ GeV}^2$ up to $N^3\text{LO}$ and for Padé [1/1] with correlated errors. In this figure our results for $N^3\text{LO}$ compared with results obtained from [6] at LO,

NLO, and $N^2\text{LO}$ QCD analysis. The shaded areas represent the fully correlated one σ statistical error bands.

In Fig. 4 we show the evolution of the valence quark distributions $xu_v(x, Q^2)$ and $xd_v(x, Q^2)$ from $Q^2 = 1 \text{ GeV}^2$

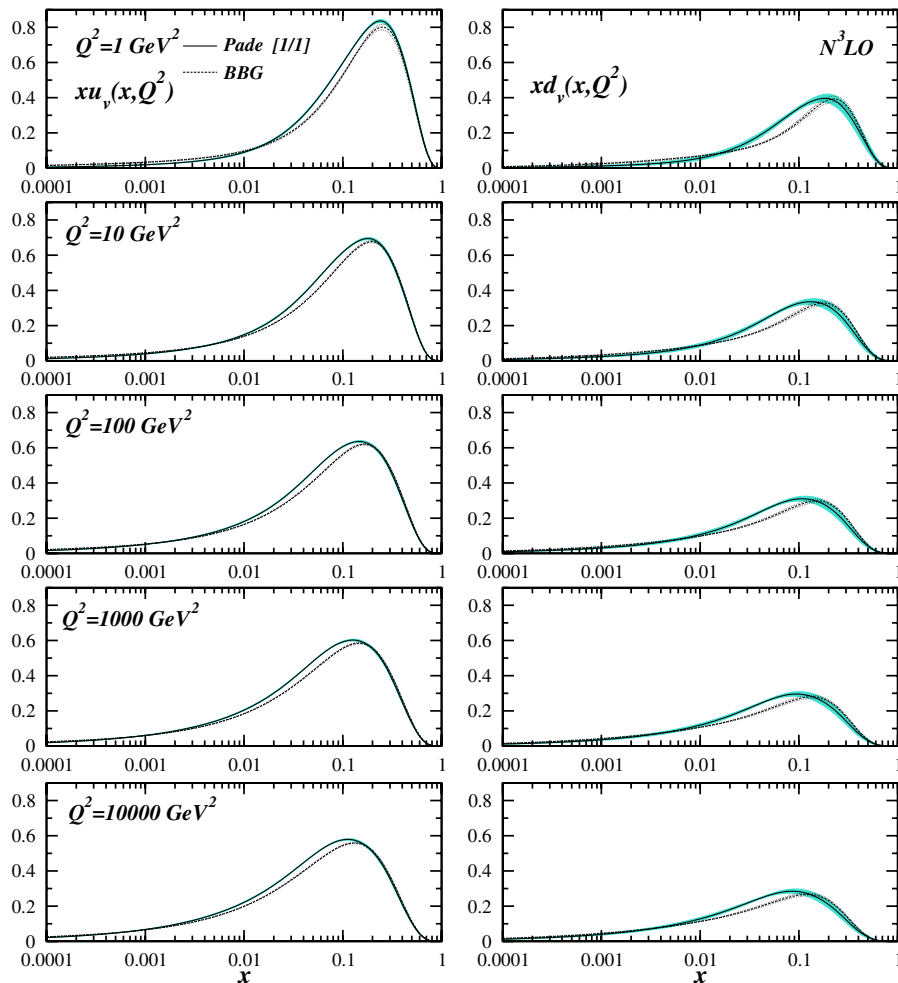


FIG. 4 (color online). The parton densities xu_v and xd_v at $N^3\text{LO}$ evolved up to $Q^2 = 10000 \text{ GeV}^2$ (solid lines) compared with results obtained by BBG (dashed line) [48].

to $Q^2 = 10^4 \text{ GeV}^2$ in the region $x \in [10^{-4}, 1]$ at $N^3\text{LO}$. In this figure we also compared our results with the nonsinglet QCD analysis from [48]. With rising values of Q^2 the distributions flatten at large values of x and rise at low values.

Another way to test the $N^3\text{LO}$ fit results is comparison of low order moments of the distributions $u_v(x, Q^2)$, $d_v(x, Q^2)$, and $u_v(x, Q^2) - d_v(x, Q^2)$. In Table III we present the lowest nontrivial moments of these distributions at $Q^2 = Q_0^2$ in $N^3\text{LO}$ and compare to the respective moments obtained for the parameterizations [48].

We should note that the unknown parameters are correlated and almost depend on the method of the QCD fits. We believe that the source of the small difference between the results of our analysis and reported results in [48] is the kind of the different method of the QCD analysis. We used the Jacobi polynomial method as an expansion method to do QCD fits but they used the exact inverse Mellin technique to obtain some unknown parameters. We also found that the results of Padé [1/1] and [0/2] in 4-loop level are almost the same.

To perform higher twist QCD analysis of the nonsinglet world data in $N^3\text{LO}$, we consider the $Q^2 \geq 4 \text{ GeV}^2$, $4 < W^2 < 12.5 \text{ GeV}^2$ cuts. The number of data points in the above range for proton and deuteron is 279 and 278, respectively. The extracted distributions for $h(x)$ in $N^3\text{LO}$ are depicted in Fig. 5 for the nonsinglet case considering scattering off the proton and deuteron target. According to our results the coefficient $h(x)$ grows towards large x . To compare, we also present the reported results of the early $N^2\text{LO}$ analysis [6] in Fig. 5. Also in this figure HT contributions have the tendency to decrease from $N^2\text{LO}$ to $N^3\text{LO}$. This effect was observed for the first time in the case of fits of F_3 DIS νN data in [13] and then studied in more detail in [15,16].

This similar effect was also observed in the fits of F_2 charge lepton-nucleon DIS data [47,48,73,74]. In Ref. [47], the functional form for $h(x)$ is chosen by

$$h(x) = a \left(\frac{x^b}{1-x} - c \right), \quad (38)$$

TABLE III. Comparison of low order moments from our nonsinglet $N^3\text{LO}$ QCD analysis at $Q_0^2 = 4 \text{ GeV}^2$ with the $N^3\text{LO}$ analysis from Ref. [48].

f	N	BBG [48]	$N^3\text{LO}$ Padé [1/1]	$N^3\text{LO}$ Padé [0/2]
u_v	2	0.3006 ± 0.0031	0.30757 ± 0.0026	0.30806 ± 0.0028
	3	0.0877 ± 0.0012	0.08771 ± 0.0011	0.08781 ± 0.0012
	4	0.0335 ± 0.0006	0.03320 ± 0.0006	0.03323 ± 0.0006
d_v	2	0.1252 ± 0.0027	0.12450 ± 0.0024	0.12495 ± 0.0025
	3	0.0318 ± 0.0009	0.03040 ± 0.0008	0.03012 ± 0.0008
	4	0.0106 ± 0.0004	0.00992 ± 0.0004	0.00993 ± 0.0005
$u_v - d_v$	2	0.1754 ± 0.0041	0.18305 ± 0.0036	0.18310 ± 0.0038
	3	0.0559 ± 0.0015	0.05767 ± 0.0013	0.05769 ± 0.0014
	4	0.0229 ± 0.0007	0.02329 ± 0.0007	0.02329 ± 0.0007

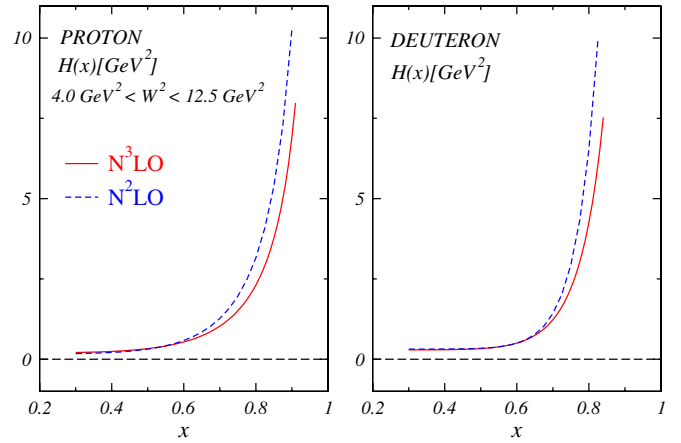


FIG. 5 (color online). The higher twist coefficient $h(x)$ for the proton and deuteron data as a function of x in $N^3\text{LO}$ (solid line) compared with results obtained by $N^2\text{LO}$ (dashed line) [6].

TABLE IV. Our results for $h(x)$ function according to Eq. (38) and for $N^3\text{LO}$.

	a	b	c
Proton	1.015	3.928	-0.193
Deuteron	4.481	7.759	-0.064

and it is possible to compare $h(x)$ results in $N^2\text{LO}$ and $N^3\text{LO}$. In Table IV we present our results for a, b, c in the above equation.

As seen from Fig. 5 $h(x)$ is widely independent of the target comparing the results for deeply inelastic scattering off protons and deuterons.

VI. DISCUSSION

A study [6] of the available world data on deep-inelastic lepton-proton and lepton-deuteron scattering provided a determination of the valence quark parton densities and α_s in wide ranges of the Bjorken scaling variable x and Q^2 up to 3-loop. In the nonsinglet case, where heavy flavor effects are negligibly small, the analysis can be extended to 4-loop level, i.e. to QCD in $N^3\text{LO}$ perturbative expansion.

The analysis was performed using the Jacobi polynomials method to determine the parameters of the problem in a fit to the data. A new aspect in comparison with previous analysis is that we determine the parton densities and the QCD scale up to N³LO by using the Jacobi polynomial expansion method and using Padé approximations. The benefit of this approach is the possibility to determine nonsinglet parton distributions analytically and not numerically. In Ref. [75] we arrange the MATHEMATICA program to extract $xu_v(x, Q^2)$ and $xd_v(x, Q^2)$ up to the 4-loops.

In this analysis we adopt the $\bar{d} - \bar{u}$ distribution at $Q_0^2 = 4 \text{ GeV}^2$ from Refs. [47,48,58,59], which gives a good description of the Drell-Yan dimuon production data [60]. The nonsinglet regime is manifesting itself at $x \geq 0.1$ as the rule. In this regime, when we changed the sea distribution from the other groups, the value of χ^2 , valence distributions, Λ , and α_s varied, but only slightly. For example, we used the $\bar{d} - \bar{u}$ distribution from [3,76–78] and we found that the value of χ^2 varies by about 3% and Λ by about 1%–2%.

In the QCD analysis we parameterized the strong coupling constant α_s in terms of four massless flavors deter-

mining Λ_{QCD} . Up to N³LO results fitting the data, are

$$\begin{aligned} \Lambda_{\text{QCD}}^{(4)} &= 213.2 \pm 28 \text{ MeV}, & \text{LO}, \\ \Lambda_{\text{QCD}}^{(4)} &= 263.8 \pm 30 \text{ MeV}, & \text{NLO}, \\ \Lambda_{\text{QCD}}^{(4)} &= 239.9 \pm 27 \text{ MeV}, & \text{N}^2\text{LO}, \\ \Lambda_{\text{QCD}}^{(4)} &= 241.4 \pm 29 \text{ MeV}, & \text{N}^3\text{LO}. \end{aligned} \quad (39)$$

These results can be expressed in terms of $\alpha_s(M_Z^2)$:

$$\begin{aligned} \alpha_s(M_Z^2) &= 0.1281 \pm 0.0028, & \text{LO}, \\ \alpha_s(M_Z^2) &= 0.1149 \pm 0.0021, & \text{NLO}, \\ \alpha_s(M_Z^2) &= 0.1131 \pm 0.0019, & \text{N}^2\text{LO}, \\ \alpha_s(M_Z^2) &= 0.1139 \pm 0.0020, & \text{N}^3\text{LO}. \end{aligned} \quad (40)$$

Note that in above results we use the matching between n_f and n_{f+1} flavor couplings calculated in Ref. [66]. We adopt this prescription to be able to compare our results with other measurements of Λ_{QCD} .

The $\alpha_s(M_Z^2)$ values can be compared with results from other QCD analysis of inclusive deep-inelastic scattering data in N²LO (see Refs. [6,15,16,41–43,47,48,79,80]).

$$\begin{aligned} \text{A02: } \alpha_s(M_Z^2) &= 0.1143 \pm 0.0014, & \text{GRS: } \alpha_s(M_Z^2) &= 0.111, & \text{MRST03: } \alpha_s(M_Z^2) &= 0.1153 \pm 0.0020, \\ \text{SY01(ep): } \alpha_s(M_Z^2) &= 0.1166 \pm 0.0013, & \text{SY01}(\nu\text{N}): \alpha_s(M_Z^2) &= 0.1153 \pm 0.0063, \\ \text{A06: } \alpha_s(M_Z^2) &= 0.1128 \pm 0.0015, & \text{BBG: } \alpha_s(M_Z^2) &= 0.1134_{-0.0021}^{+0.0019}, & \text{BM07: } \alpha_s(M_Z^2) &= 0.118 \pm 0.0019, \\ \text{KPS00}(\nu\text{N}): \alpha_s(M_Z^2) &= 0.118 \pm 0.002 \text{ (stat)} \pm 0.005 \text{ (syst)} \pm 0.003 \text{ (theory)}, \\ \text{KPS03}(\nu\text{N}): \alpha_s(M_Z^2) &= 0.119 \pm 0.002 \text{ (stat)} \pm 0.005 \text{ (syst)} \pm 0.002 \text{ (threshold)}_{-0.002}^{+0.004} \text{ (scale)}, \\ \text{KT08: } \alpha_s(M_Z^2) &= 0.1131 \pm 0.0019. \end{aligned}$$

The N³LO values of $\alpha_s(M_Z^2)$ can also be compared with results from other QCD analysis [48],

$$\text{BBG: } \alpha_s(M_Z^2) = 0.1134_{-0.0021}^{+0.0019},$$

and with the value of the world average, 0.1189 ± 0.0010 [81], and the current world average,

$$\alpha_s(M_Z^2) = 0.1184 \pm 0.0007, \quad (41)$$

which has been extracted in [82] very recently. It seems that our results confirm that the value of $\alpha_s(M_Z^2)$ from DIS turns out to be sizably below the world average. In this case, it would be useful to find out which set of data is mainly responsible for the low value of $\alpha_s(M_Z^2)$. We will try to see which subset makes $\alpha_s(M_Z^2)$ particularly small in a future work.

We hope our results of QCD analysis of structure functions in terms of Jacobi polynomials could be able to

describe more complicated hadron structure functions. We also hope to be able to consider massive quark contributions by using the structure function expansion in terms of the Jacobi polynomials.

ACKNOWLEDGMENTS

We are especially grateful to G. Altarelli for guidance and critical remarks. A. N. K. is grateful to F. Olness and J. Blümlein for useful discussions and constructive comments. H. K. is grateful to S. Moch for his guidance and discussion. We would like to thank Z. Karamloo and M. Ghominejad for reading the manuscript of this paper. A. N. K. is grateful to TH-PH division at CERN for their hospitality while he visited there and amended this paper. A. N. K. thanks Semnan University for partial financial support of this project. We acknowledge the School of Particles and Accelerators, Institute for Research in Fundamental Sciences (IPM) for financially supporting this project.

- [1] G. Altarelli, arXiv:0907.1751.
- [2] <http://indico.cern.ch/conferenceOtherViews.py?view=standard&confId=43022>.
- [3] A. D. Martin, W. J. Stirling, R. S. Thorne, and G. Watt, *Eur. Phys. J. C* **63**, 189 (2009).
- [4] R. S. Thorne, *Nucl. Phys. B, Proc. Suppl.* **191**, 295 (2009).
- [5] P. M. Nadolsky *et al.*, *Phys. Rev. D* **78**, 013004 (2008).
- [6] A. N. Khorramian and S. A. Tehrani, *Phys. Rev. D* **78**, 074019 (2008).
- [7] I. S. Barker, B. R. Martin, and G. Shaw, *Z. Phys. C* **19**, 147 (1983); I. S. Barker and B. R. Martin, *Z. Phys. C* **24**, 255 (1984); S. P. Kurlovich, A. V. Sidorov, and N. B. Skachkov, *JINR Report No. E2-89-655*, 1989.
- [8] G. Parisi and N. Sourlas, *Nucl. Phys.* **B151**, 421 (1979); I. S. Barker, C. B. Langensiepen, and G. Shaw, *Nucl. Phys.* **B186**, 61 (1981).
- [9] V. G. Krivokhizhin, S. P. Kurlovich, V. V. Sanadze, I. A. Savin, A. V. Sidorov, and N. B. Skachkov, *Z. Phys. C* **36**, 51 (1987).
- [10] V. G. Krivokhizhin *et al.*, *Z. Phys. C* **48**, 347 (1990).
- [11] J. Chyla and J. Rames, *Z. Phys. C* **31**, 151 (1986).
- [12] I. S. Barker, C. S. Langensiepen, and G. Shaw, *Nucl. Phys.* **B186**, 61 (1981).
- [13] A. L. Kataev, A. V. Kotikov, G. Parente, and A. V. Sidorov, *Phys. Lett. B* **417**, 374 (1998).
- [14] A. L. Kataev, G. Parente, and A. V. Sidorov, arXiv:hep-ph/9809500.
- [15] A. L. Kataev, G. Parente, and A. V. Sidorov, *Nucl. Phys.* **B573**, 405 (2000).
- [16] A. L. Kataev, G. Parente, and A. V. Sidorov, *Phys. Part. Nucl.* **34**, 20 (2003); *Nucl. Phys. B, Proc. Suppl.* **116**, 105 (2003).
- [17] A. N. Khorramian, S. Atashbar Tehrani, and M. Ghominejad, *Acta Phys. Pol. B* **38**, 3551 (2007).
- [18] A. N. Khorramian and S. A. Tehrani, *J. Phys. Conf. Ser.* **110**, 022022 (2008).
- [19] A. N. Khorramian and S. A. Tehrani, *AIP Conf. Proc.* **1006**, 118 (2008).
- [20] S. Atashbar Tehrani and A. N. Khorramian, *Nucl. Phys. B, Proc. Suppl.* **186**, 58 (2009).
- [21] A. N. Khorramian, S. Atashbar Tehrani, H. Khanpour, and S. Taheri Monfared, *Hyperfine Interact.* **194**, 337 (2009).
- [22] A. N. Khorramian, S. Atashbar Tehrani, M. Soleymaninia, and S. Batebi, *Hyperfine Interact.* **194**, 341 (2009).
- [23] S. Atashbar Tehrani and A. N. Khorramian, *Hyperfine Interact.* **194**, 331 (2009).
- [24] S. Atashbar Tehrani and A. N. Khorramian, *Appl. Math. Inf. Sci.* **3**, 367 (2009).
- [25] E. Leader, A. V. Sidorov, and D. B. Stamenov, *Int. J. Mod. Phys. A* **13**, 5573 (1998).
- [26] S. Atashbar Tehrani and A. N. Khorramian, *J. High Energy Phys.* **07** (2007) 048.
- [27] A. N. Khorramian and S. Atashbar Tehrani, arXiv:0712.2373.
- [28] A. N. Khorramian and S. Atashbar Tehrani, *AIP Conf. Proc.* **915**, 420 (2007).
- [29] A. Mirjalili, A. N. Khorramian, and S. Atashbar-Tehrani, *Nucl. Phys. B, Proc. Suppl.* **164**, 38 (2007).
- [30] A. Mirjalili, S. Atashbar Tehrani, and A. N. Khorramian, *Int. J. Mod. Phys. A* **21**, 4599 (2006).
- [31] A. C. Benvenuti *et al.* (BCDMS Collaboration), *Phys. Lett. B* **237**, 592 (1990); **223**, 485 (1989); **237**, 592 (1990); **237**, 599 (1990).
- [32] L. W. Whitlow, E. M. Riordan, S. Dasu, S. Rock, and A. Bodek, *Phys. Lett. B* **282**, 475 (1992).
- [33] M. Arneodo *et al.* (New Muon Collaboration), *Nucl. Phys.* **B483**, 3 (1997).
- [34] C. Adloff *et al.* (H1 Collaboration), *Eur. Phys. J. C* **21**, 33 (2001); **30**, 1 (2003).
- [35] J. Breitweg *et al.* (ZEUS Collaboration), *Eur. Phys. J. C* **7**, 609 (1999); S. Chekanov *et al.* (ZEUS Collaboration), *Eur. Phys. J. C* **21**, 443 (2001).
- [36] M. A. Samuel, J. Ellis, and M. Karliner, *Phys. Rev. Lett.* **74**, 4380 (1995).
- [37] J. Ellis, E. Gardi, M. Karliner, and M. A. Samuel, *Phys. Lett. B* **366**, 268 (1996).
- [38] J. Ellis, E. Gardi, M. Karliner, and M. A. Samuel, *Phys. Rev. D* **54**, 6986 (1996).
- [39] G. A. Baker, Jr., *Essentials of Padé Approximants* (Academic, New York, 1975).
- [40] C. M. Bender and S. A. Orszag, *Advanced Mathematical Methods for Scientists and Engineers* (McGraw-Hill, New York, 1978).
- [41] A. D. Martin, R. G. Roberts, W. J. Stirling, and R. S. Thorne, arXiv:hep-ph/0307262.
- [42] S. Alekhin, *Phys. Rev. D* **68**, 014002 (2003).
- [43] J. Santiago and F. J. Yndurain, *Nucl. Phys.* **B611**, 447 (2001).
- [44] A. L. Kataev, G. Parente, and A. V. Sidorov, *Nucl. Phys. B, Proc. Suppl.* **116**, 105 (2003); *Fiz. Elem. Chastits At. Yadra* **34**, 43 (2003) [*Phys. Part. Nucl.* **34**, 20 (2003)].
- [45] J. Santiago and F. J. Yndurain, *Nucl. Phys.* **B563**, 45 (1999).
- [46] J. Blümlein, H. Böttcher, and A. Guffanti, *Nucl. Phys. B, Proc. Suppl.* **135**, 152 (2004); arXiv:hep-ph/0606309.
- [47] M. Glück, E. Reya, and C. Schuck, *Nucl. Phys.* **B754**, 178 (2006).
- [48] J. Blumlein, H. Böttcher, and A. Guffanti, *Nucl. Phys.* **B774**, 182 (2007).
- [49] S. Alekhin, J. Blumlein, S. Klein, and S. Moch arXiv:0908.2766 [*Phys. Rev. D* (to be published)], and references therein.
- [50] W. L. van Neerven and A. Vogt, *Nucl. Phys.* **B568**, 263 (2000).
- [51] W. L. van Neerven and A. Vogt, *Nucl. Phys.* **B588**, 345 (2000).
- [52] J. Blümlein and A. Vogt, *Phys. Rev. D* **58**, 014020 (1998).
- [53] M. Glück, C. Pisano, and E. Reya, *Eur. Phys. J. C* **50**, 29 (2007).
- [54] J. A. M. Vermaseren, A. Vogt, and S. Moch, *Nucl. Phys.* **B724**, 3 (2005).
- [55] V. Barone, M. Genovese, N. N. Nikolaev, E. Predazzi, and B. G. Zakharov, *Z. Phys. C* **58**, 541 (1993).
- [56] J. Kwiecinski and B. M. Badelek, *Z. Phys. C* **43**, 251 (1989).
- [57] P. Amaudruz *et al.* (New Muon Collaboration), *Phys. Rev. Lett.* **66**, 2712 (1991); M. Arneodo *et al.* (New Muon Collaboration), *Phys. Rev. D* **50**, R1 (1994); *Nucl. Phys.* **B487**, 3 (1997).
- [58] A. D. Martin *et al.*, *Eur. Phys. J. C* **23**, 73 (2002).
- [59] J. Blümlein, H. Böttcher, and A. Guffanti, *Nucl. Phys. B, Proc. Suppl.* **135**, 152 (2004).

- [60] R. S. Towell *et al.* (E866 Collaboration), *Phys. Rev. D* **64**, 052002 (2001).
- [61] W. Furmanski and R. Petronzio, *Z. Phys. C* **11**, 293 (1982).
- [62] W.L. van Neerven and E.B. Zijlstra, *Phys. Lett. B* **272**, 127 (1991); E.B. Zijlstra and W.L. van Neerven, *Nucl. Phys.* **B383**, 525 (1992).
- [63] O. V. Tarasov, A. A. Vladimirov, and A. Y. Zharkov, *Phys. Lett.* **93B**, 429 (1980).
- [64] S. A. Larin and J. A. M. Vermaseren, *Phys. Lett. B* **303**, 334 (1993).
- [65] A. Vogt, *Comput. Phys. Commun.* **170**, 65 (2005).
- [66] K. G. Chetyrkin, B. A. Kniehl, and M. Steinhauser, *Phys. Rev. Lett.* **79**, 2184 (1997); S. Bethke, *J. Phys. G* **26**, R27 (2000); W. Bernreuther and W. Wetzel, *Nucl. Phys.* **B197**, 228 (1982); **B513**, 758(E) (1998).
- [67] W. A. Bardeen, A. J. Buras, D. W. Duke, and T. Muta, *Phys. Rev. D* **18**, 3998 (1978).
- [68] K. Abe *et al.* (E143 Collaboration), *Phys. Lett. B* **452**, 194 (1999).
- [69] G. Parisi and N. Surlas, *Nucl. Phys.* **B151**, 421 (1979).
- [70] D. Stump *et al.*, *Phys. Rev. D* **65**, 014012 (2001).
- [71] F. James, *CERN Program Library Long Writeup D506: MINUIT* (CERN, Geneva, 1994).
- [72] H. Georgi and H. D. Politzer, *Phys. Rev. D* **14**, 1829 (1976).
- [73] U. K. Yang and A. Bodek, *Eur. Phys. J. C* **13**, 241 (2000).
- [74] J. Blumlein and H. Bottcher, *Phys. Lett. B* **662**, 336 (2008).
- [75] Program summary at <http://particles.ipm.ir/links/QCD.htm>.
- [76] M. Gluck, P. Jimenez-Delgado, and E. Reya, *Eur. Phys. J. C* **53**, 355 (2008).
- [77] A. D. Martin, W. J. Stirling, R. S. Thorne, and G. Watt, *Phys. Lett. B* **652**, 292 (2007).
- [78] P. Jimenez-Delgado and E. Reya, *Phys. Rev. D* **79**, 074023 (2009).
- [79] S. Alekhin, K. Melnikov, and F. Petriello, *Phys. Rev. D* **74**, 054033 (2006).
- [80] P. M. Brooks and C. J. Maxwell, *Nucl. Phys.* **B780**, 76 (2007).
- [81] S. Bethke, *Prog. Part. Nucl. Phys.* **58**, 351 (2007).
- [82] S. Bethke, *Eur. Phys. J. C* **64**, 689 (2009).